Colloidosomes Hot Paper

International Edition: DOI: 10.1002/anie.201501615
German Edition: DOI: 10.1002/ange.201501615

Electrostatic Assembly/Disassembly of Nanoscaled Colloidosomes for Light-Triggered Cargo Release**

*Song Li, Basem A. Moosa, Jonas G. Croissant, and Niveen M. Khashab**

Abstract: *Colloidosome capsules possess the potential for the encapsulation and release of molecular and macromolecular cargos. However, the stabilization of the colloidosome shell usually requires an additional covalent crosslinking which irreversibly seals the capsules, and greatly limits their applications in large-cargos release. Herein we report nanoscaled colloidosomes designed by the electrostatic assembly of organosilica nanoparticles (NPs) with oppositely charged surfaces (rather than covalent bonds), arising from different contents of a bridged nitrophenylene-alkoxysilane [NB; 3-nitro-N-(3-(triethoxysilyl)propyl)-4-(((3-(triethoxysilyl)-propyl)-amino)methyl)benzamid] derivative in the silica. The surface charge of the positively charged NPs was reversed by light irradiation because of a photoreaction in the NB moieties, which impacted the electrostatic interactions between NPs and disassembled the colloidosome nanosystems. This design was successfully applied for the encapsulation and light-triggered release of cargos.*

Colloidosomes can be formed by the assembly of colloidal particles on emulsion droplets leading to capsule morphologies.[1–5] Various colloidal nanobuilding blocks have been used to design colloidosomes such as iron oxide NPs,[6] nanodiamonds,[7] polymeric rod-shaped microparticles,[8] silica NPs,[9,10] cubic metal–organic frameworks NPs,[11] and mixtures of these NPs.[9,10] The key interest of such structures is their important internal volume combined with the properties of the nanobuilding blocks in the shell, which promise many applications as witnessed by few pioneering studies involving enzyme encapsulation,[12,13] bacteria encapsulation,[14] biocatalysis,[3] and passive release or delivery by interparticle pores.[15–17]

Colloidal NPs assemble at the interface of emulsion droplets during the colloidosome formation in order to decrease interfacial energy of the system.[18] The assembly at the liquid–liquid interface requires that particles should be neither completely wetted by the oil phase nor by the aqueous phase.[19] To adjust the wettability of NPs, the hydrophobization of the surface of colloids is usually carried out. This can be achieved by physical interactions with additives (e.g. surfactants),[7,9,20] or chemical functionalization.[21,22] Typically, colloidal particles with partially hydrophobic surfaces, such as silica NPs functionalized with organosilane,[23,24] are chosen as nanobuilding blocks of colloidosomes. These colloidal NPs assemble at the oil/water (o/w) or water/oil (w/o) interfaces of emulsion droplets,[17] which is much analogous to the behavior of surfactants.

Many applications of colloidosomes are nonetheless compromised by several challenges such as the stability of the hollow structure and the accessibility of the internal volume. Controlled release and delivery applications require that the colloidosome carriers be: (1) stabilized after the emulsion stage,[17] (2) non-permeable to ensure the transportation of the loaded active entities in cells, (3) able to release and deliver on-demand their payload,[25–27] and (4) nanoscaled ($8 <$ size < 800 nm) to benefit from the enhanced permeation and retention effect.[9,28,29] First, the synthesis of stable colloidosomes requires the additional crosslinking or "irreversible locking" of the NP building blocks forming the shell to ensure the stability of the structure during solvent transfer and drying steps, as well as further applications.[1] This was usually done by sintering polymeric NPs,[15,30] polymerizing the droplet phase,[17] trapping of an aqueous gel,[31] or covalent cross-linking.[12,17] Silica NPs were crosslinked by additional condensation of a silica layer to stabilize the colloidosomes.[24,32,33] A Glycerol functionalization was used to covalently crosslink silica colloidosomes.[34] Layered polyelectrolytes were also prepared to stabilize the nanobuilding blocks.[1,35,36] Subsequently to silica crosslinking, a pH-responsive copolymer polyelectrolyte was covalently linked to hundred micrometer-large silica colloidosomes to vary the extent of the permeation of dye cargos.[33] Unfortunately the formation of covalently bonded layers renders such capsules irreversibly assembled, which is undesirable for the release of cargos larger that the interparticle pores. The second challenge is to prevent the passive leakage of entities present within the colloidosomes, which usually occurs through the interparticle pores. Multiple layers of colloidosomes were thus developed to minimize this phenomenon.[23,24] Notably, controlled double layer of silica colloidosomes were assembled with a thin silica layer in between to seal the system.[23,24] However, the application of colloidosomes in transportation and release of molecular and macromolecular cargos relies both on the ability prevent the passive leakage and to disassemble on demand the hollow structure. To our knowledge, the ability to controllably release cargos using colloidosomes was not reported. Concerning the size requirement, though few recent findings report nanoscaled colloidosomes,[7,9,20] most colloidosomes are microcapsules

[*] S. Li, B. A. Moosa, J. G. Croissant, Prof. N. M. Khashab
Smart Hybrid Materials (SHMs)
Advanced Membranes and Porous Materials Center
King Abdullah University of Science and Technology (KAUST)
Thuwal 23955-6900 (KSA; Saudi Arabia)
E-mail: niveen.khashab@kaust.edu.sa

[**] We gratefully acknowledge support from King Abdullah University of Science and Technology (KAUST).

Supporting information for this article is available on the WWW under http://dx.doi.org/10.1002/anie.201501615.

typically ranging from one to a hundred micrometer in diameter. Thus, reported colloidosomes do not meet essential criteria of release and delivery applications.

Herein we employ for the first time electrostatic interactions between negatively and positively charged nitrophenylene-doped silica nanoparticles (NBSN-1 and NBSN-2, respectively) to form stable nanoscaled colloidosomes that are efficiently disassembled upon light exposure due to charge reversal of NBSN-2 (see Figure 1). Given the negative

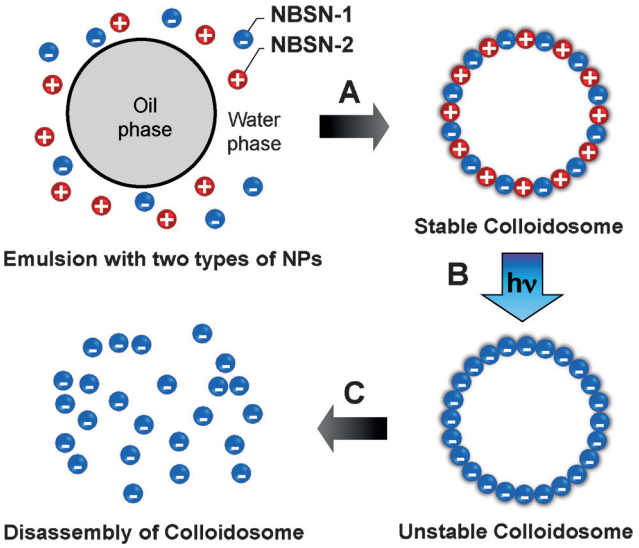

Figure 1. A) Schematic illustration of colloidosomes made from oppositely charged organosilica NPs (NBSN-1 and 2) in o/w emulsion. B,C) Light-triggered colloidosome disassembly by the charge reversal of NBSN-2.

charge of silica at pH 7, a higher content of a positively charged nitrophenylene-ammonium-bridged alkoxysilane (NB, Figure 2A) in NBSN-2 than in NBSN-1 afforded a positive surface charge in the former NPs. The NBSN were efficiently used to form colloidosome nanocapsules without further covalent crosslinking. Furthermore, the photoreaction of NB moieties in the NBSN-2 framework induced the NPs charge reversal and subsequent disassembly of the colloidosomes due to electrostatic repulsions. The unique electrostatic disassembly feature of the designed colloidosomes was applied for light-triggered cargo release.

The photosensitive nitrophenylene-ammonium-bridged alkoxysilane derivative was first synthesized and characterized. Two equivalent of 3-(aminopropyl)triethoxysilane were reacted with one equivalent of 4-(bromomethyl)-3-nitrobenzoic acid (see Figure S1 in the Supporting Information) in order to produce the photosensitive NB precursor (see Figure 2A). The design of NB was demonstrated by ^{1}H and ^{13}C nuclear magnetic resonance (NMR) spectra (Figure S2).

The photoresponsiveness of this precursor was studied and monitored by UV/Vis and NMR spectroscopies (see Figure 2B and Figure S3 respectively). In accordance with the abundant literature, we propose that upon illumination the cleavage of the benzyl in ortho of the nitrophenylene moiety in NB leads to aminopropyl and nitrosobenzaldehyde alkoxysilane fragments, which then react in a classical organic reaction to produce the imine alkoxysilane (see Figure 2B). Indeed, the NB molecule is analogous to *o*-nitrobenzyl ether[37,38] and *o*-nitrobenzyl thioether[39,40] which are known to photocleave in nitrosobenzaldehyde molecules. Spectroscopically, the cleavage of the benzyl bond generated a gradual increase of the band at 350 nm characteristic of aldehydes, while the original peak at 223 nm shifted to 238 nm and kept increasing, reflecting the change of functionalities attached to the phenyl ring of the precursor.[37,40] This is consistent with the clear disappearance of the singlet of the benzyl group at 4.1 ppm observed by proton NMR spectroscopy (Ph-CH_2-NH-; see Figure S3),[41] and the shift of the nitro stretching vibration mode in the Fourier transform infrared spectra due to the production of nitroso functions (Figure S4). Comparing the increased absorbance (ΔA) with the baseline (A_0) at 350 nm, the ratio $\Delta A/A_0$ could be used to monitor the completion of the photoreaction (see Figure S5). The photoreaction process was found to be quantitative after 10 minutes.

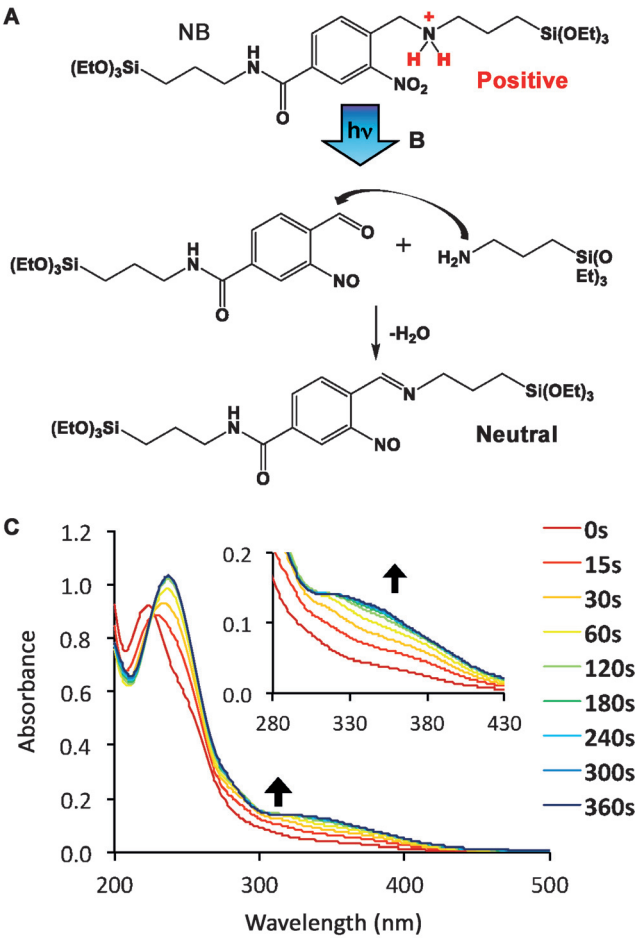

Figure 2. A) Structure of the designed positively charged NB alkoxysilane precursor, and B) the proposed photocleavage mechanism generating nitrobenzaldehyde and aminopropyl alkoxysilane derivatives which then reacts to form the neutral imine alkoxysilane. C) Absorbance spectra of NB overtime upon irradiation at 365 nm in absolute ethanol.

NB-doped silica NPs were then synthesized, and their morphology and composition were characterized. The nanomaterials were designed by precise control of the reaction conditions via co-condensation of the NB precursor and tetraethoxysilane with ammonia catalyst in a modified Stöber process (see the Supporting Information).[42–44] To achieve a higher NB organic content in NBSN-2 than in NBSN-1 the only requirement was to conduct the sol–gel process for a longer time because of a lower condensation kinetic of the bridged alkoxysilane (48 vs. 24 h). Transmission and scanning electron microscopy (TEM, SEM) images revealed 100 nm organosilica nanospheres for both syntheses (see Figure 3 and

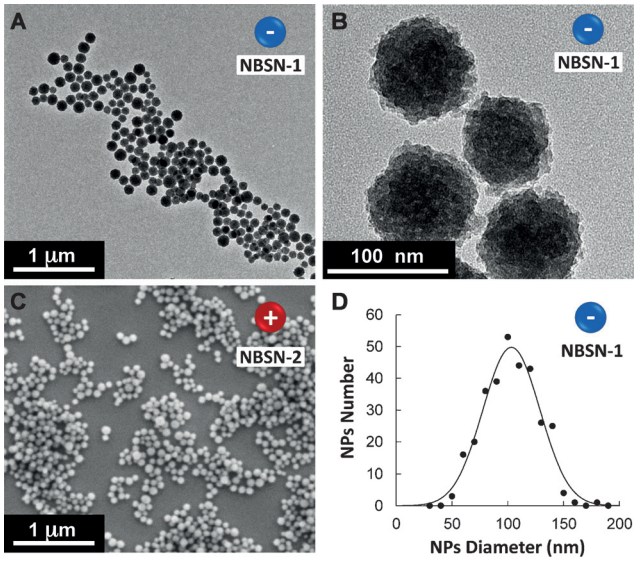

Figure 3. A,B) TEM micrographs of NBSN-1, and C) SEM micrograph of NBSN-2. D) NBSN-1 size distribution determined from statistical analysis of TEM data of 400 NPs.

Figure S6). NBNS-1 and 2 nanomaterials were nearly monodisperse NPs as displayed by the narrow size distribution and non-aggregated (Figure 3D and Figure S6D), which is paramount to a proper colloidosome assembly. The organic–inorganic hybrid composition of the NPs was confirmed by UV/Vis spectra of NBSN-1 and 2, both display absorption at 230 nm characteristic of the benzene derivative of the NB moieties (Figure S7). The NB content in NBSN-1 and 2 were determined by elemental analysis of nitrogen in the NPs and were found to be of 10 and 33%, respectively (see Table S1). The carbon over nitrogen experimental ratio also corresponded to the incorporation of the NB moieties within the silica framework.

The surface charge of NBSN was investigated in view of their electrostatic nanoassembly. Zeta potential measurements at neutral pH on NBSN-1 revealed a negative charge of surface (−52 mV), while NBSN-2 showed a slightly positive charge of surface (+15 mV, see white bars in Figure 4). In a control experiment with silica NP (SN) prepared with a similar Stöber method (see the Supporting Information), a more negatively charged surface was obtained (−81 mV; see white bar in Figure 4). These results are consistent with the

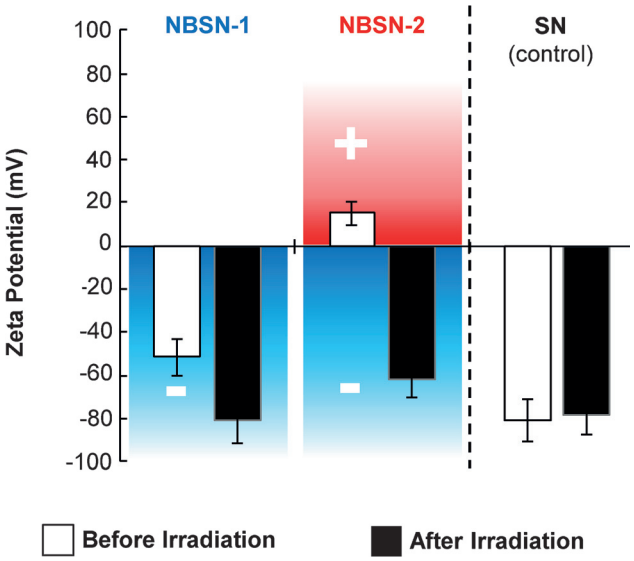

Figure 4. Zeta-potential measurements at pH 7 for NBSN compounds, and for SN control before and after after irradiation 10 minutes at 365 nm. Erros bars are calculated from three measurements.

higher incorporation of positively charged NB moieties in NBSN-2, which overcomes the silanolates negative charges. The influence of the pH on the surface charge of the NBSN-1 and 2 was studied between pH 5 and 9, and both NPs were found to respectively remain negatively and positively charged (see Figure S8A). Additionally, the surface of NBSN nanobuilding blocks exhibited UV-photoresponsiveness. After 10 minutes of laser irradiation at 365 nm, irradiated NBSN-2 displayed a charge reversal (from +15 to −62 mV, see Figure 4) arising from the NB photoreaction in the NPs matrix which eventually affords the neutral imine groups. Hence, the surface charge of NBSN-1 became more negative (from −52 to −81 mV, see black bar Figure 4), which was similar to that of SN. This phenomenon was clearly assigned to the NB photoreaction in the NPs, as shown by the trend observed overtime in the UV/Vis spectra (see Figure S9), which is identical to that of the molecular precursor (Figure 2C). The spectroscopic data thus strongly suggest that the photoreaction of NB moieties bearing protonated secondary amine function, leads to NPs with surface charges mainly governed by silanolates.

These two nanobuilding blocks were then used for the design of colloidosomes in o/w emulsion. In a typical procedure, NBSN-1 and 2 were mixed in water at pH 8 and this solution was used as continuous phase to disperse aliquots of toluene. The o/w mixture was emulsified by sonication (125 W cm^{-2}) for 30 minutes, and then stirred gently for 1 h to stabilize the system without the need of further crosslinking (the Supporting Information).[23,32] The resulting colloidosomes were characterized by SEM, which demonstrated the stabilization of the aesthetic colloidosome nanoassembly (see Figure 5A,B and Figure S10). Besides, the hollow structure of these capsules formed by a monolayer of organosilica NPs could be observed by TEM micrographs (Figure 5C and S11), as well as by SEM in the rare case of a partially opened colloidosome (Figure 5D). Moreover, the colloidosomes

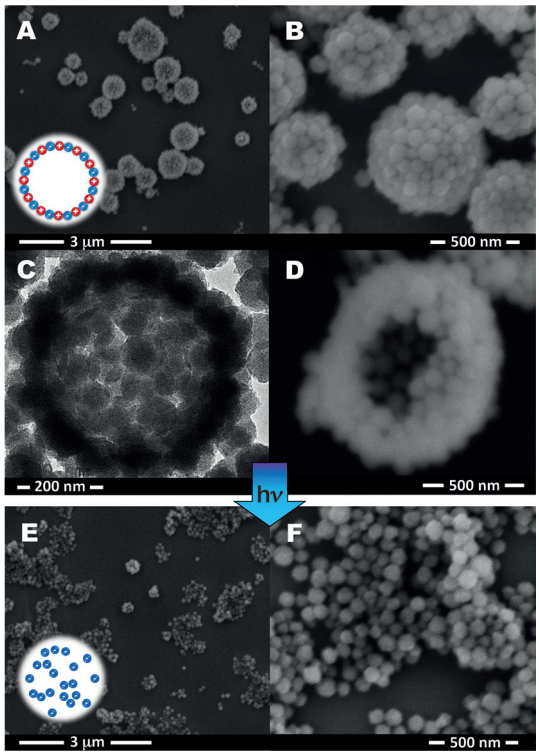

Figure 5. A,B,D) SEM micrographs of colloidosomes designed by electrostatic interactions in o/w emulsion. C) TEM image of one colloidosme nanoassembly. E,F) SEM images of the disassembled colloidosomes after 10 minutes of irradiation at 365 nm.

were surprisingly small, with sizes ranging from 200 to 700 nm, unlike most systems of micron scales. The average hydrodynamic diameter of the colloidosome nanosystems was assessed to be of 413 nm by dynamic light scattering (DLS) measurements (Figure S12), which is consistent SEM micrographs (Figure S10). The formation of these colloidosomes was governed by two factors: (1) electrostatic interactions to stabilize the structure, and (2) the partial hydrophobicity of organosilica hybrid NPs. Consequently, when on the one hand only one type of charged NP was used (NBSN-1 or 2), the colloidosomes formation was not favored (Figure S13 A–D). On the other hand, when negatively charged SN and a control of positively charged aminopropyl-functionalized silica NPs ($SN\text{-}NH_2$) were used to design colloidosomes, the lack partial hydrophobicity in NPs did not allow either the stable nanoassembly at the o/w interface (Figure S13 E,F). Hence, NBSN-1 and 2 were uniquely suited for the fabrication of stable colloidosomes.

The light-responsiveness of the colloidosomes nanosystems was then investigated. A colloidosomes aqueous solution was irradiated as previously carried with the UV laser at 365 nm, and SEM analysis was performed. As expected, the irradiation of the colloidosomes caused their disassembly as clearly shown by SEM micrographs after light exposure (see Figure 5 E,F). This conclusion was supported by the measured charge reversal of NBSN-2 at this pH after irradiation (Figure S8), which results in charge repulsion between NBSN building blocks. Note that, consistently with the electrostatic assembly/disassembly mechanism, the deprotonation of the ammonium group at pH 11 induced the pH-triggered disassembly of the colloidosomes (see Figure S15). This is the first reported study on a controlled disassembly of stable colloidosomes.

The colloidosome nanoplatforms featuring an on-demand electrostatically driven assembly/disassembly were then applied as nanocarriers for cargo release. The Nile Red dye was used for its good solubility in toluene and the emulsification was performed according to the initial conditions (see the Supporting Information). Light-induced disassembly cycles were performed for 5 minutes at 365 nm by turning on and off the laser. The release of the dye was monitored by UV/Vis spectroscopy (Figure S14) and plotted as a function of time (Figure 6). Before irradiation, the flat baseline indicated

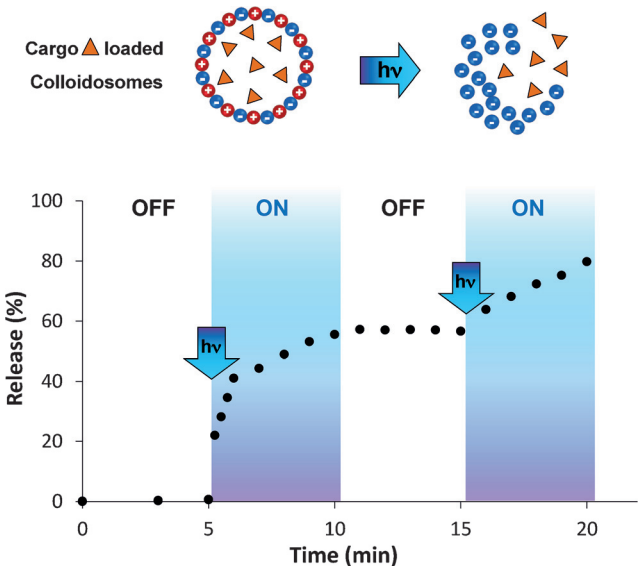

Figure 6. Light-induced release of encapsulated Nile Red dye in colloidosomes (365 nm laser). The on/off cycles of 5 minutes correlate the cargo release. The last point corresponds to the release maximum.

the absence of passive release from the colloidosome nanocarriers. However, when the light was shown 5 minutes on the dispersion, the colloidosomes became unstable and 60 % of cargos were released (Figure 6). Given the symmetry of the irradiation (Figure S14) and the fact that 10 minutes are needed for a complete photoreaction (Figure S5), 20 % of encapsulated dyes molecules could then be released from the colloidosomes when the illumination was turned on again for 5 minutes. Nearly 80 % of encapsulated dyes could be released in such experimental conditions and the release profile plot was not hindered by a photobleaching of the dye (Figure S16).

In conclusion, we have demonstrated the successful design of organosilica colloidosome at the nanoscale by electrostatic interactions without additional covalent crosslinking. The incorporation of a positively charged bridged organo-alkoxysilane in different amount in silica NPs enabled the adjustment of the surface charge in order to have either negatively or positively charged nanobuilding blocks with a partial

hydrophobicity. Furthermore, the photoresponsiveness of the organic part constituting organosilica NPs was harnessed to disassemble on demand the colloidosomes by charge reversal of the positively charged building blocks. This unique feature was applied for the controlled release of cargos upon light actuation, which we envision for the transportation and release of hydrophobic molecules, as well as very large macromolecules and nanoparticles, which is a key advantage in comparison to most porous capsules with internal volume only accessible to relatively small cargos.

Keywords: colloidosomes · emulsions · organosilica compounds · release · silica nanoparticles

How to cite: *Angew. Chem. Int. Ed.* **2015**, *54*, 6804–6808
Angew. Chem. **2015**, *127*, 6908–6912

[1] A. D. Dinsmore, M. F. Hsu, M. G. Nikolaides, M. Marquez, A. R. Bausch, D. A. Weitz, *Science* **2002**, *298*, 1006–1009.
[2] F. Li, D. P. Josephson, A. Stein, *Angew. Chem. Int. Ed.* **2011**, *50*, 360–388; *Angew. Chem.* **2011**, *123*, 378–409.
[3] Z. Wang, M. C. M. van Oers, F. P. J. T. Rutjes, J. C. M. van Hest, *Angew. Chem. Int. Ed.* **2012**, *51*, 10746–10750; *Angew. Chem.* **2012**, *124*, 10904–10908.
[4] G. Stephenson, R. M. Parker, Y. Lan, Z. Yu, O. A. Scherman, C. Abell, *Chem. Commun.* **2014**, *50*, 7048–7051.
[5] J. S. Sander, A. R. Studart, *Langmuir* **2013**, *29*, 15168–15173.
[6] B. Samanta, D. Patra, C. Subramani, Y. Ofir, G. Yesilbag, A. Sanyal, V. M. Rotello, *Small* **2009**, *5*, 685–688.
[7] M. Maas, T. Bollhorst, R. N. Zare, K. Rezwan, *Part. Part. Syst. Charact.* **2014**, *31*, 1067–1071.
[8] P. F. Noble, O. J. Cayre, R. G. Alargova, O. D. Velev, V. N. Paunov, *J. Am. Chem. Soc.* **2004**, *126*, 8092–8093.
[9] T. Bollhorst, S. Shahabi, K. Wörz, C. Petters, R. Dringen, M. Maas, K. Rezwan, *Angew. Chem.* **2015**, *127*, 120–125.
[10] X.-W. Xu, X.-M. Zhang, C. Liu, Y.-L. Yang, J.-W. Liu, H.-P. Cong, C.-H. Dong, X.-F. Ren, S.-H. Yu, *J. Am. Chem. Soc.* **2013**, *135*, 12928–12931.
[11] M. Pang, A. J. Cairns, Y. Liu, Y. Belmabkhout, H. C. Zeng, M. Eddaoudi, *J. Am. Chem. Soc.* **2013**, *135*, 10234–10237.
[12] P. H. Keen, N. K. Slater, A. F. Routh, *Langmuir* **2014**, *30*, 1939–1948.
[13] C. Zhang, C. Hu, Y. Zhao, M. Möller, K. Yan, X. Zhu, *Langmuir* **2013**, *29*, 15457–15462.
[14] P. H. R. Keen, N. K. H. Slater, A. F. Routh, *Langmuir* **2012**, *28*, 16007–16014.
[15] H. N. Yow, A. F. Routh, *Langmuir* **2009**, *25*, 159–166.
[16] F. Porta, A. Kros, *Part. Part. Syst. Charact.* **2013**, *30*, 606–613.
[17] K. L. Thompson, M. Williams, S. P. Armes, *J. Colloid Interface Sci.* **2014**, http://dx.doi.org/10.1016/j.jcis.2014.11.058.
[18] Z. Niu, J. He, T. P. Russell, Q. Wang, *Angew. Chem. Int. Ed.* **2010**, *49*, 10052–10066; *Angew. Chem.* **2010**, *122*, 10250–10265.
[19] A. R. Studart, U. T. Gonzenbach, I. Akartuna, E. Tervoort, L. J. Gauckler, *J. Mater. Chem.* **2007**, *17*, 3283–3289.
[20] T. Bollhorst, T. Grieb, A. Rosenauer, G. Fuller, M. Maas, K. Rezwan, *Chem. Mater.* **2013**, *25*, 3464–3471.
[21] M. Li, D. C. Green, J. L. R. Anderson, B. P. Binks, S. Mann, *Chem. Sci.* **2011**, *2*, 1739–1745.
[22] R. K. Kumar, M. Li, S. N. Olof, A. J. Patil, S. Mann, *Small* **2013**, *9*, 357–362.
[23] J. S. Sander, A. R. Studart, *Soft Matter* **2014**, *10*, 60–68.
[24] H. Wang, X. Zhu, L. Tsarkova, A. Pich, M. Möller, *ACS Nano* **2011**, *5*, 3937–3942.
[25] S. Shilpi, A. Jain, Y. Gupta, S. K. Jain, *Crit. Rev. Ther. Drug Carrier Syst.* **2007**, *24*, 361–391.
[26] K. K. Cotí, M. E. Belowich, M. Liong, M. W. Ambrogio, Y. A. Lau, H. A. Khatib, J. I. Zink, N. M. Khashab, J. F. Stoddart, *Nanoscale* **2009**, *1*, 16–39.
[27] J. Croissant, A. Chaix, O. Mongin, M. Wang, S. Clément, L. Raehm, J.-O. Durand, V. Hugues, M. Blanchard-Desce, M. Maynadier, A. Gallud, M. Gary-Bobo, M. Garcia, J. Lu, F. Tamanoi, D. P. Ferris, D. Tarn, J. I. Zink, *Small* **2014**, *10*, 1752–1755.
[28] J. Croissant, M. Maynadier, A. Gallud, H. P. N′Dongo, J. L. Nyalosaso, G. Derrien, C. Charnay, J.-O. Durand, L. Raehm, F. Serein-Spirau, N. Cheminet, T. Jarrosson, O. Mongin, M. Blanchard-Desce, M. Gary-Bobo, M. Garcia, J. Lu, F. Tamanoi, D. Tarn, T. M. Guardado-Alvarez, J. I. Zink, *Angew. Chem. Int. Ed.* **2013**, *52*, 13813–13817; *Angew. Chem.* **2013**, *125*, 14058–14062.
[29] H.-M. Song, J. I. Zink, N. M. Khashab, *Part. Pat. Syst. Charact.* **2015**, *32*, 307–312.
[30] L. Yang, X. Ge, M. Wang, L. Song, X. He, *Mater. Lett.* **2008**, *62*, 429–431.
[31] O. J. Cayre, P. F. Noble, V. N. Paunov, *J. Mater. Chem.* **2004**, *14*, 3351–3355.
[32] Y. Zhao, Y. Li, D. E. Demco, X. Zhu, M. Möller, *Langmuir* **2014**, *30*, 4253–4261.
[33] M. Li, R. L. Harbron, J. V. M. Weaver, B. P. Binks, S. Mann, *Nat. Chem.* **2013**, *5*, 529–536.
[34] L. A. Fielding, S. P. Armes, *J. Mater. Chem.* **2012**, *22*, 11235–11244.
[35] V. D. Gordon, X. Chen, J. W. Hutchinson, A. R. Bausch, M. Marquez, D. A. Weitz, *J. Am. Chem. Soc.* **2004**, *126*, 14117–14122.
[36] D. B. Lawrence, T. Cai, Z. Hu, M. Marquez, A. D. Dinsmore, *Langmuir* **2007**, *23*, 395–398.
[37] Y. V. Il′ichev, M. A. Schwörer, J. Wirz, *J. Am. Chem. Soc.* **2004**, *126*, 4581–4595.
[38] M. Smet, L.-X. Liao, W. Dehaen, D. V. McGrath, *Org. Lett.* **2000**, *2*, 511–513.
[39] G. Delaittre, T. Pauloehrl, M. Bastmeyer, C. Barner-Kowollik, *Macromolecules* **2012**, *45*, 1792–1802.
[40] G. Liu, C.-M. Dong, *Biomacromolecules* **2012**, *13*, 1573–1583.
[41] T. Mes, R. van der Weegen, A. R. A. Palmans, E. W. Meijer, *Angew. Chem. Int. Ed.* **2011**, *50*, 5085–5089; *Angew. Chem.* **2011**, *123*, 5191–5195.
[42] W. Stöber, A. Fink, E. Bohn, *J. Colloid Interface Sci.* **1968**, *26*, 62–69.
[43] A. van Blaaderen, A. P. M. Kentgens, *J. Non-Cryst. Solids* **1992**, *149*, 161–178.
[44] L. Tang, T. M. Fan, L. B. Borst, J. Cheng, *ACS Nano* **2012**, *6*, 3954–3966.

Received: February 18, 2015
Revised: March 19, 2015
Published online: April 27, 2015

